Copy 3

PROGRESS REPORT - 1/15/61 - 2/15/61

CONTRACT NO. AF 33(600)40280

SYNCHRONIZER

Frequency Generator

The preliminary design of the frequency generator was finished and the schematic and parts list was completed. The parts list does not include special R-F coil drawing numbers as these will have to be worked out on the breadboard and assigned new drawing numbers later.

The "varicap" (voltage-variable silicon capacitors) design for the modulator section has been determined and proven feasible. Preliminary data indicate a modulator sensitivity of nearly twice the design goal. Drawing number 576R654 has been assigned to "varicaps".

C&M has released our specifications (on the oscillator and discriminator) to purchasing on 2/9/61. Delivery of one breadboard and 2 prototypes will take approximately 12 weeks so that the frequency generator design cannot be proven before 10 May 1961. The oscillator and discriminator together will cost approximately $1200.00 per set for final models as well as for the breadboard and prototype units.

Sync-Generator

The design and preliminary testing of this unit is completed. Schematic and parts list have also been completed. A borrowed jitter tester will be available soon for a preliminary look at the inherent jitter on the sync-gen output pulses. Jitter is expected to be greater than originally anticipated because the original gating design was found unworkable with the high clock frequency used.

Effort is now directed toward the final physical configuration of these circuits using printed circuit techniques. When the "breadboard" printed circuit boards have been proven satisfactory, the design will be given to drafting for duplication.

Oscillator units for the breadboard are on order and are due on 10 March 1961. Cost for this item is $332.00 per unit.

STALO

Measurements made upon the borrowed STALO units have shown the frequency deviations at 400 cps and 800 cps are excessive. Deviations due to light shocks were found to be considerably greater under 80 cps modulating frequencies than at greater modulating frequencies. These measurements were taken without vibration isolators. The D.C. amplifier drifts were found to be within limits as long as the 400 cps line voltage varied less than 1%. A D.C. amplifier with more gain and theoretically more stable with respect to line variations and cathode emission has been built, and will be checked out.

Negotiations are being made to obtain 3 stalo units from production. These then are to be modified in the model shop for the production units.

NAVIGATION TIE-IN

A servo amplifier unit has been obtained. A gear assembly to which the geared servo-motor, geared step-motor and two control potentiometers are mounted is being designed and constructed. Negotiations are being made to purchase a step-motor with an appropriate gear box. A parts list and a schematic has been completed.

RECEIVER

A "Will Ship" date of 2/22/61 has been received for the traveling wave tube. A 30 mc receiver was obtained and checked out for use in testing the TWT noise figure. Other test equipment including a TWT power supply will be ready by 2/24/61.

The IF amplifier schematic was completed and parts list made and a breadboard layout started. The video amplifier schematic was started. It was decided that the synchronous mixer should be moved from the IF amplifier to the video amplifier for better impedance matching and for lower cable losses. Two double balanced synchronous mixers have been designed and constructed, one using 6688 miniature pentodes and the other employing 7077 ceramic triodes. Both have undergone some testing. Because of the space saving advantage of using the ceramic triodes the circuit utilizing them has received the most attention.

Problems were encountered in attenuating the L.O. signal in the detector output and also in obtaining the required frequency response. In the circuit using the 6688 pentodes the attenuation of the L.O. in the output was marginally satisfactory without any attempt to provide additional filtering. The frequency response of this detector was not yet adequate when work on it was discontinued. In the detector employing the 7077 triodes a series resonant trap was required in the output to obtain sufficient attenuation of the L.O. signal. Work is presently continuing to obtain the desired frequency response in this circuit.

As part of this work it was necessary to design, construct, and test a 120 mc power amplifier which is used with a signal generator to provide the L.O. signal of proper amplitude.

A receiver failure detector circuit, which is compatible with the system failure monitor, was designed, breadboarded and tested. This circuit, consisting of two transistors and four resistors, will be included in the video amplifiers and will detect the loss of receiver noise. The circuit will be tied in to the failure light on the control panel such that the light comes on if noise is lost.

POWER SUPPLY - CONTROL PANEL

A revised quote has been received from Components Section. Two quotes have been received from outside suppliers. Three outside suppliers have not quoted, but are expected to quote and will have these quotes in to Westinghouse by 2/20/61. Approximately eight other outside suppliers sent a "no bid" answer.

The turn on procedure has been completely revised and most of the components for this procedure have been determined.

A tentative parts list and schematic for the power supply have been completed.

A tentative parts list and schematic for the control panel has been completed. A sketch of the layout of the control panel has been made and this sketch is waiting approval before being placed in drafting.

"C" requests have been placed with Components Section for two switches on the Control Panel and also to put four of [redacted] filament transformers on to Westinghouse drawings.

25X1

25X1

MODULATOR

The design of the control panel and controlling sequence required some changes in the modulator. It was decided that additional interlocks such as klystron heater current, modulator pressure and other interlocks on the R-T would be used on the modulator high voltage. These changes were incorporated in the modulator design.

Drafting is proceeding on the modulator. The trigger generator layout has been completed. The filter box layout is complete and detailing under way. Layout of the complete modulator is nearly complete.

Construction of the first breadboard is proceeding. The ceramic thyratron and inverse diode have been received. The PFN, charging choke, pulse transformer, high voltage power supply and klystron heater transformer will not be received for about 2 months. Pending their receipt, a high voltage supply, PFN and charging choke from another radar are being used in the modulator breadboard. Checkout of the triggering stability of the klystron and the inverse diode operation can be checked with these substitutes and as the new components are received they can be incorporated.

RESONANT RING

25X1

In conjunction with [redacted] it was determined that the 1/3 height dump switch is not suitable for this application, i.e. it is too lossy unfired, and does not present a good short, or fast rise times, in the fired condition.

SECRET

Work was resumed with the full height waveguide switch, and several significant results were obtained, due mainly to the high power available from the 4J50 modulator:

(1) With constant power in the ring, rise time of output pulse increases 4 to 1 as the gap increases from 2/64 to 5/64 with trigger voltage a 3 KV.

(2) Increasing trigger voltage will decrease rise time.

(3) With trigger voltage constant, and RF incident at switches just below the self-breakdown value for each gap spacing, rise time increases 2 to 1 as the gap increased from 2/64 to 5/64.

(4) Hold-off of 180 KW peak in the ring was attained, with a rise time of 2.5 nanosec, at a gap spacing of 4/64.

Control drawing and a PDS for the final ring were completed. They and the DD254 necessary for transmittal to suppliers have been submitted for supplier concurrence and quotation.

The design of directional couplers, power monitors, etc., were completed and purchase part drawings completed where necessary.

The waveguide preasurization necessary for final system was determined and drawings requested for necessary pressure switches to prevent unpressurized operation.

SWITCH TUBES

A tube was constructed in which a trigger electrode was inserted, and at the same time triggering circuitry and H.V. power supplies were assembled to supply a trigger pulse. The trigger pulse could be positioned.

with respect to the R.F. pulse. Switching action obtained was not satisfactory. Rise time of the pulse appeared to be slow (approx. 50 NS) and switching was achieved roughly 50% of the time. Tests were repeated for changes in pressure but with the same result.

One major difficulty with the trigger electrode in this tube (and also the succeeding tube) is that the gap spacing cannot be adjusted. A readily adjustable gap will be desirable on future tubes.

A design has been made for a tube which can be controlled by a magnetic field. A coil design was investigated that offers the possibility of obtaining a pulsed magnetic field with NS rise times. Parts for this tube and its pulsing circuitry are presently being made and assembled.

ANTENNA

Electrical

Manifold - Tests on various manifold test pieces are currently under way. These pieces are those needed to check out specifically the design of manifold number 3 or 5. It is expected that this manifold design will be released by 2-16-61 for fabrication by a technique such as electro forming. The complete manifold is too complex to fabricate by ordinary metal working techniques; an electro formed part will provide a low cost unit for complete design evaluation as well as evaluation of the electro forming process. This unit will be as representative a final configuration as possible and if suitable may be useable as an end use item.

Array - The decision to change the vertical aperture from 19.5" to 11" has been made. Factors considered in this decision are stated in a special adendum to this report (Vertical Antenna Pattern Considerations). Sample 21" sticks have been evaluated for radiation patterns, VSWR, and power radiated. The design has been revised for 11" sticks. Evaluation of the 21" model indicates that more slots (on alternate sides of the centerline) are needed. This slot configuration introduces possible problems with mutual coupling which must be evaluated. An experiment on a single slot in an 11" waveguide to determine the individual slot characteristics is under way.

A study to evaluate the effects of side lobes upon the overall system has been completed and is attached as an addendum to this report. (Antenna Side Lobe Effects in Side Looking Doppler Radars). It would indicate the system is rather tolerant of the antenna pattern.

Tolerance Study - Computer runs for the far field radiation pattern of the 131 element array with optimum support locations as a function of various values of EI were made (modulus of elasticity of the honeycomb X Inertia). It was determined that a value of EI of $26.1 \times 10^6$ would be required to attain a 19.5 db sidelobe level for a nominally 25 db array. The results of this phase of the study (in particular the honeycomb requirements versus weight) are presently being discussed between the responsible project group and the antenna section.

Radome - Methods for measuring dielectric constants on the flexible samples have been evaluated. Tests are currently under way, using what appears to be a method valid for random thickness, low loss samples.

Load - Several heat tests were conducted on 3 load materials at 600°F for several hours. No physical deterioration of any sample occurred. The most promising load sample (Custom Components, Inc.) was electrically monitored through the run. A VSWR variation of 1.05:1 was noted. The sample started at $_{1}$ and reached 1.05 x $_{1}$ at 300-400° and maintained this value until the heat was removed. The evaluation indicated that the variation was due to mounting changes rather than material change. An half height load sample is now being obtained to further evaluate mounting methods.

Mechanical

Structure Analysis - The honeycomb beam was redesigned to accommodate the 11" array. A sketch of the redesigned beam and its mounting facilities has been submitted to O Section for their information and to obtain approval of the outline dimensions and mounting points. Discussions with several prospective suppliers have taken place and a few suggestions for improved manufacturability were made. The anticipated costs are now approximately $7,500 per panel.

Manifold Design - The mechanical configuration of the manifold has been completed and drafting is completing a sketch. A test piece

will be electroformed from this sketch and final drawings will be made from this sketch after the successful testing of the prototype. The lowest cost estimate for electroforming the manifolds, miters, transitions, and array sticks has been received from Technicraft. They have been invited to present detailed proposals as to method of manufacture and delivery schedule.

Array Design and Power Dividers - Electroforming has been selected as the most reasonable means of manufacturing the array sticks. The costs of slotting the sticks by the electrical discharge method proved to be excessive. The costs of milling the slots plus the difficulties of deburning made this method as costly or more costly than electroforming. The array sticks have been redesigned to the 11" array requirement, incorporating mounting features and load mounting provisions. The approximated cost is $16,600 for the 384 sticks.

The thermal expansion differential between the stainless steel honeycomb and the nickel waveguide indicate a necessity of inserting sections of flexible waveguide into each portion of the power divider.

Tolerance Study - A new computer run has been made to determine RF deterioration due to bending; using a beam of maximum thickness (faces of .070). One of the factors affecting bending is that of temperature difference across the antenna thickness. It is elaborated upon in an addendum to this report (Antenna Pattern - Effect of Thermal Deflections). If this deterioration is within acceptable limits, the honeycomb beam as designed could be used. If not within acceptable limits, additional thickness

of antenna structure will be necessary. Approximately 25 lbs of weight could be saved by increasing the honeycomb thickness (and overall thickness) by 3/4 of an inch and reducing the face thickness to .040. However, this would cause the antenna to exceed its thickness specification by 3/4 of an inch.

Radome Design - Thermal aging of samples of adhesives and laminates continues. Four laminates and approximately eight adhesives have survived the tests so far. Bonding tests have been initiated to determine the actual bonding characteristics of several combinations of adhesive and laminate against nickel. Bonding, sealing, thermal and pressure tests will be made as soon as tensile tests, on cured bonding test samples, have been completed.

Load and Seals - Investigations into "O" rings and pressure windows have been made to determine materials necessary, cost and availability.

Load configu ation and mounting provisions have been determined and are awaiting PF design completion before having drawings made.

WESTINGHOUSE ELECTRIC CORPORATION

CURVE NO.

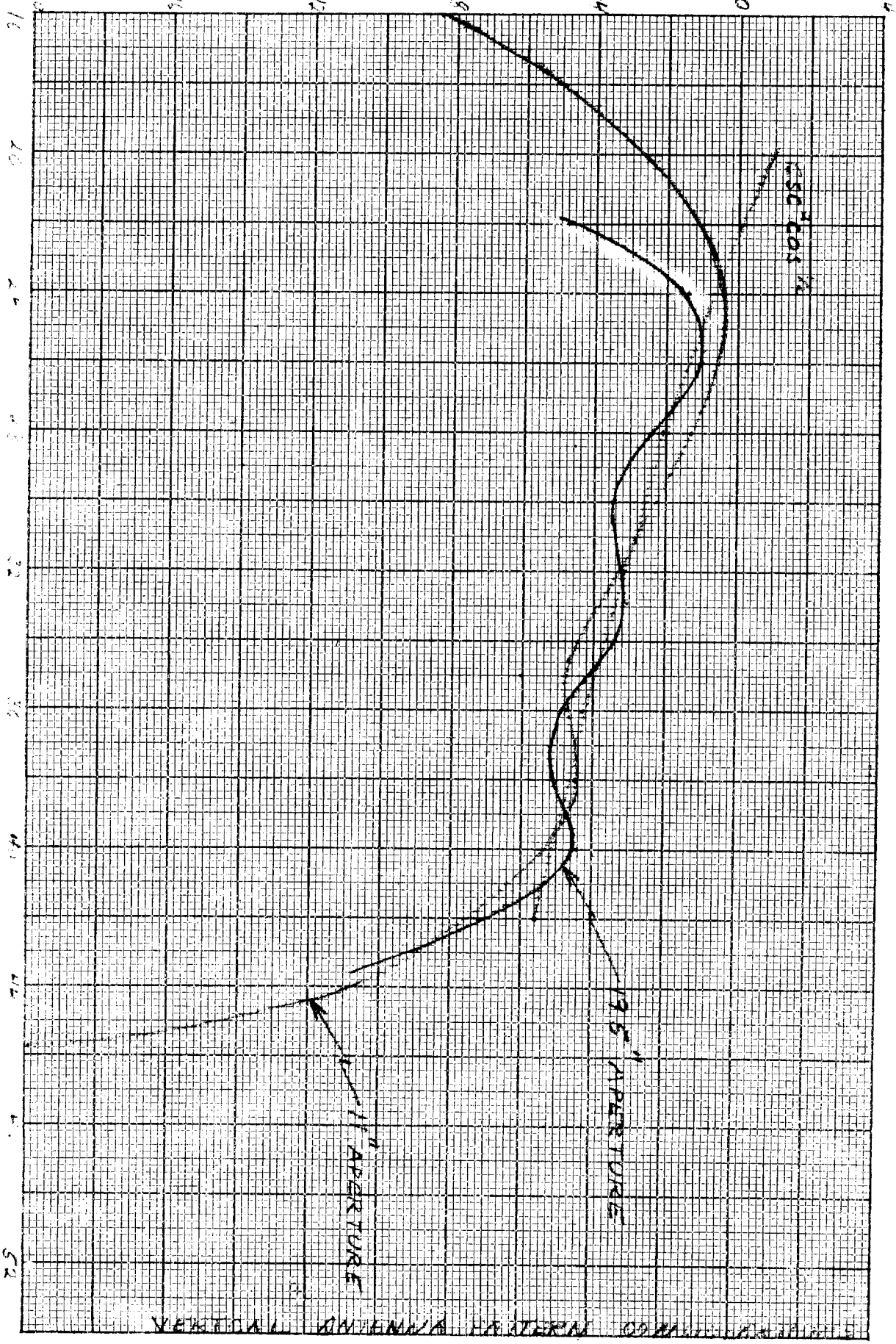


VERTICAL ANTENNA PATTERN

FIGURE 2

## VERTICAL ANTENNA PATTERN CONSIDERATIONS

Design investigation has disclosed that approximately 100 lbs weight in the antenna could be saved if the vertical aperture was reduced from 19.5 inches to 11 inches. It was computed that this could be accomplished with a reduction of gain from 35.4 db to 34.9 db. The following investigationwas made to consider the effects of the resulting change in the vertical antenna pattern. These considerations and conclusions can also apply to the problem of "altitude line" effects.

To determine the effects of skirt shape of the antenna pattern on the return signal, it is useful to consider the timing sequence shown in Figure 1.

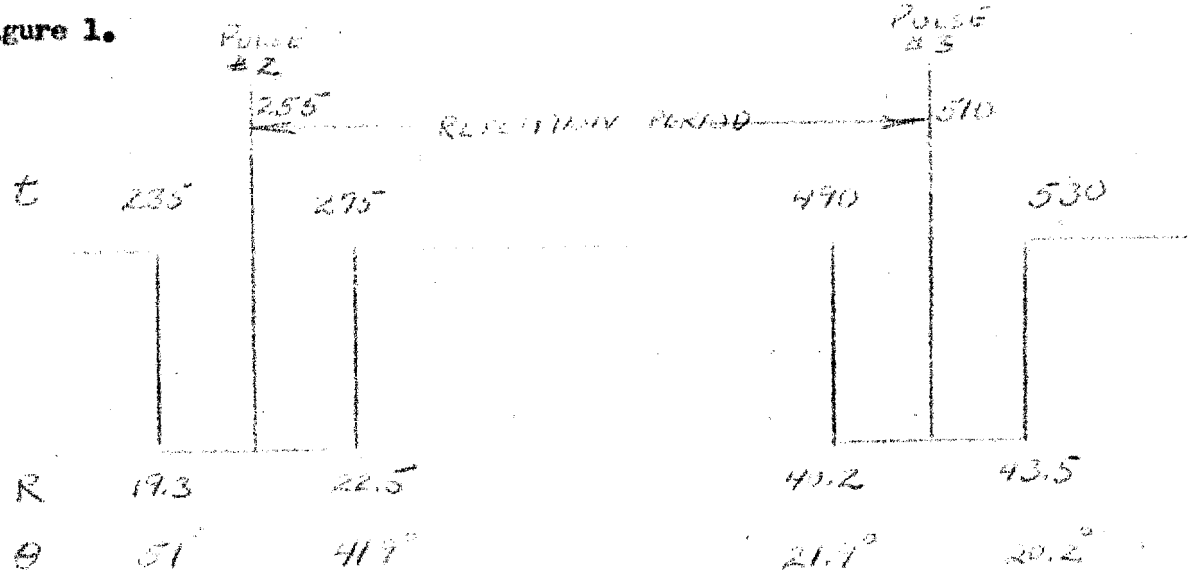


Figure 1

From the antenna pattern curves, Figure 2, it can be seen that a return coming from a 51° depression angle is more than 40 db below the $\csc^2$ $\cos^{\frac{1}{2}}$ pattern, since there is over 20 db loss each way. Thus it can be seen that there is no problem from "first time around echo".

At 20.2° depression angle, however, the 11 inch antenna pattern is only 2.6 db below the $\csc^2 \cos^{\frac{1}{2}}$ pattern, giving a return 5.2 db down. (Note that the 19 inch antenna gives a return only 10 db down). Thus the rejection of "third time around echo" depends for the most part on the coherent integration factor. Assuming a coherent integration factor of 20.3 db at the near range (including a 2 db loss factor) a target at 22.5 miles would be enhanced 20.3 db. The target at 43.5 miles, however, would be enhanced 3 db by the focusing action, but attenuated 3 db by the aperture shaping. Thus the difference between desired and undesired targets would be 25.5 db for the 11 inch antenna and 30.3 db for the 19 inch antenna.

The conclusion drawn from this is that no significant penalty is paid for use of the 11 inch antenna.

## ANTENNA PATTERN - EFFECT OF THERMAL DEFLECTIONS

The SOARD antenna will show a tendency to bow due to differential expansion of the two faces of the honeycomb structure when a thermal gradient exists across the honeycomb. This discussion attempts to evaluate the problem in terms of allowable temperature difference and heat flow.

Neglecting end effects the differential expansion will cause the antenna to assume a circular shape. The amount of bow, b in Figure 1 can be written as

$$b = \frac{(L/2)^2}{2R} = \frac{L^2}{8R} \qquad (1)$$

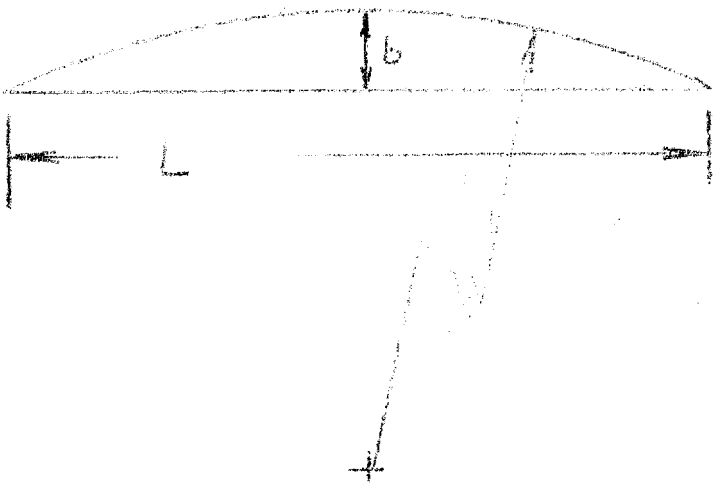


Considering the detailed view of Figure 2, we can write the relationship between inner and outer face length as

$$\theta = \frac{L}{R} = \frac{L + \Delta L}{R + t} = \frac{\Delta L}{t} \qquad (2)$$

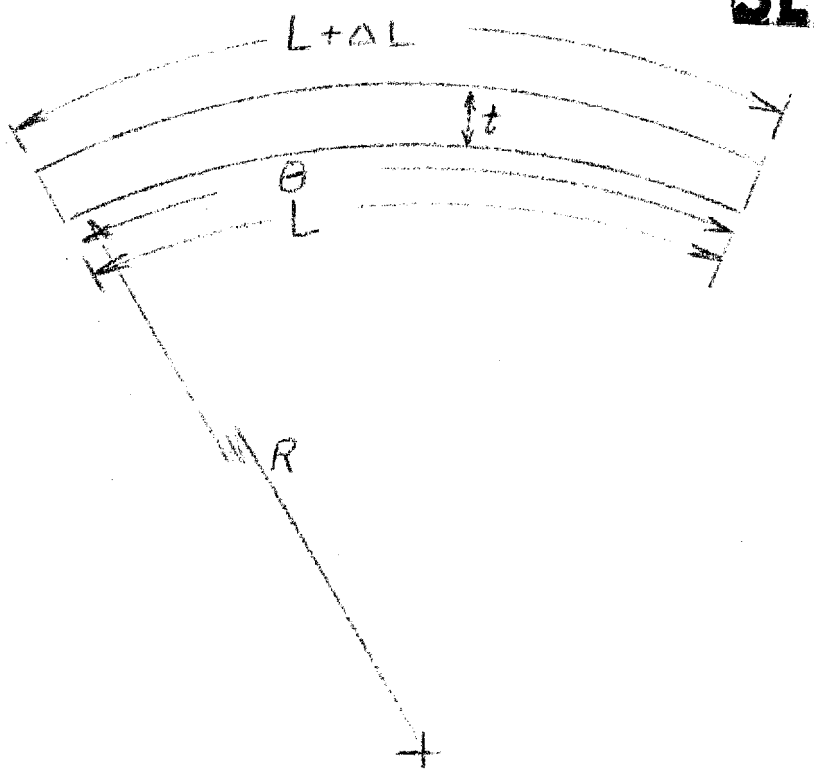


Substituting $\frac{\Delta L}{t}$ for $\frac{L}{R}$ in (1) yields

$$b = \frac{L \Delta L}{8t} \qquad (3)$$

A further substitution that can be made is to write $\Delta L$ in terms of the thermal expansion coefficient, L $\Delta$ T. Thus, the amount of bow is

$$b = \frac{L^2 \quad T}{8t} \qquad (4)$$

Substituting L = 132 in, $\quad = 10^{-5}/°C$, t = 1.5 in, and $\Delta T = 1°C$, the numerical amount bow is 0.0145 in/°C.

The total allowable deflection from the mean in an antenna is somewhere between $\pm \frac{\quad}{8}$ and $\pm \frac{\quad}{16}$, from all causes. Arbitrarily assigning $\pm \frac{\quad}{20}$ as the bow due to thermal effects makes b equal to $\frac{\quad}{10}$ or 0.12 in. Thus a temperature difference of 8°C is allowable between faces.

To relate this to heat flow, it is necessary to deduce a heat transfer coefficient for honeycomb material. The assumption made here is that heat transfer is a combination of conduction and radiation in proportion to the relative cross sections of metal and space in the material.

Radiated power may be computed from

$$Pr = 37\ e \times 10^{-12} \left[(T + \Delta T)^4 - (T)^4\right] \text{ watts/in}^2 \qquad (5)$$

Expanding $Pr = 37\ e \times 10^{-12} \left[4T^3 \Delta T + 6T(\Delta T)^2 + 4T(\Delta T)^3 + (\Delta T)^4\right]$ (5a)

or $Pr = 37\ e \times 10^{-12} \times 4T^3 \Delta T\left[1+1.5\frac{\Delta T}{T} + \left(\frac{\Delta T}{T}\right)^2 + 0.25\left(\frac{\Delta T}{T}\right)^3\right]$ (5b)

Since T is on the order of 533° K values of $\Delta T$ on the order of 10°C or less will permit dropping all the terms of (5b) containing $\frac{\Delta T}{T}$.

Substituting T =533°K, $\Delta T$ = 1°C, and e = 0.2, (assuming some roughness of the interior surfaces of the face plates caused by brazing), the value of Pr comes out to 0.00448 watts/in$^2$°C.

Stainless steel has a conductivity of 15 BTU ft/hr ft$^2$°F. A piece 1.5 inches thick will conduct 0.44 watts/in$^2$°C.

The honeycomb has a cell size 0.25 x 0.25, with 0.0015 inch material. The cross section is therefore 1.2% metal and 98.8% space.

Applying these factors to the above conductivity figures, the metal conducts 0.00528 watts/in$^2$°C and the spaces radiate 0.00443 watts/in$^2$°C. The total is 0.00971 watts/in$^2$°C. For 8°C, we have 0.0777 watts/in$^2$ or 38.2 BTU/ft$^2$ hr allowable heat flow.

The conclusion reached is that the rate of heat flow through the antenna must be limited by suitable insulation, including insulated mounts, to keep the thermal deflection within tolerable limits.

Weapons Systems Technical Memorandum No. 225

# ANTENNA SIDE LOBE EFFECTS IN SIDE-LOOKING DOPPLER RADARS

by

25X1

January 23, 1961

ABSTRACT

REPORT No. WSTM 225 DATE 1/23/61 PAGES 11

TITLE ANTENNA SIDE LOBE EFFECTS IN SIDE-LOOKING DOPPLER RADARS

CLASSIFICATION: REPORT Confidential ABSTRACT* Confidential

ABSTRACT:

Expressions are developed relating antenna side lobe structure to synthetic pattern structure in side-looking doppler radars. The synthetic main beam appears quite insensitive to antenna side lobes. Antenna side lobe power at angular equivalents of prf harmonics is important and produces synthetic pattern side lobes. These synthetic pattern side lobes have magnitudes approximately equal to the square of the average antenna side lobe level.

*ABSTRACT SHOULD BE UNCLASSIFIED IF AT ALL POSSIBLE

AE65A

UNITERMS

Side-Looking
Doppler Radar
Side-Lobes

AUTHOR(S)

25X1

## Introduction

The objective of this calculation is to obtain an estimate of the relation between physical antenna pattern structure and synthetic antenna pattern structure in a side-looking doppler radar. In particular, the effects of antenna side lobes and sampling are of primary interest.

It is convenient to express all relevant quantities in terms of the angle off the normal to the line of flight, $\Theta$ . This angle may be related to the time variable by means of the relation

$$\Theta = \frac{Vt}{R} \tag{1}$$

$\theta$ = angle off the normal to vehicle line of flight

$V$ = vehicle velocity

$R$ = range

$t$ = time

The following notation is adopted:

$G(\theta)$ = antenna gain pattern

$D(\theta)$ = doppler pattern

$S(\theta)$ = sampling function

The signal received from a target moving through the beam will simply be the product of these three quantities. This product will be called the aperture function and denoted by $A(\Theta)$.

$$A(\theta) = G(\theta)D(\theta)S(\theta) \tag{2}$$

The function $S(\Theta)$ is periodic and can be represented by a Fourier series. The doppler pattern, although not periodic, is oscillatory. Their product has the form of a harmonic series. In the signal processing operation, it is only the fundamental component of this series which is significant. This fundamental component is denoted by $\overline{A(\Theta)}$.

In the signal processing operation, the function $\overline{A(\Theta)}$ is employed as an aperture function in a coherent optical system. The power distribution in image space or the synthetic gain pattern may be expressed as

$$P(\theta_1) \sim \left| \int \overline{A(\theta)} W(\theta - \theta_1) e^{iK'(\theta-\theta_1)^2} d\theta \right|^2 \tag{3}$$

An internally generated aperture weighting function, W( ), is employed which is matched to the main beam portion of the antenna pattern for optimum performance. The constant $K^{-1}$ is adjusted to yield a maximum output from one of the doppler components. We now proceed to the detailed specification of the factors composing $\overline{A(\theta)}$ and the evaluation of the integral above.

The Doppler Pattern and Sampling Function

The doppler pattern will be of the following general form:

$$D(\theta) \sim \cos(K\theta^2 + \varphi) \tag{4}$$

$$K = \frac{2\pi R}{\lambda} \tag{5}$$

The sampling function is represented as a sequence of narrow sampling pulses separated by the angular equivalent of the repetition period. A Fourier series representation of such a function will be of the following form:

$$S(\theta) \sim 1 + 2\cos 2K\theta_0\theta + 2\cos 4K\theta_0\theta + \cdots \tag{6}$$

The parameter $\theta_0$ will have the following relation to the prf, $f_r$

$$\theta_0 = \frac{\lambda}{2V} f_r \tag{7}$$

The product of $D(\theta)$ and $S(\theta)$ will now be

$$\begin{aligned} D(\theta)S(\theta) \sim{}& \cos(K\theta^2+\varphi) + \cos(K(\theta-\theta_0)^2 - K\theta_0^2 + \varphi) \\ &+ \cos(K(\theta+\theta_0)^2 - K\theta_0^2 + \varphi) + \cdots \end{aligned} \tag{8}$$

Only the first three terms of this series will be of significance in this analysis. The aperture function, $A(\theta)$, is thus

$$A(\theta) \sim G(\theta)\left(\cos(K\theta^2+\varphi) + \cos(K(\theta-\theta_0)^2 - K\theta_0^2+\varphi) + \cos(K(\theta+\theta_0)^2 - K\theta_0^2+\varphi)\right) \tag{9}$$

The fundamental component is

$$A(\theta) \sim \begin{cases} G(\theta)\cos(K(\theta+\theta_0)^2 - K\theta_0^2 + \varphi), & -\frac{3\theta_0}{2} < \theta < -\frac{\theta_0}{2} \\ G(\theta)\cos(K\theta^2+\varphi), & -\frac{\theta_0}{2} < \theta < \frac{\theta_0}{2} \\ G(\theta)\cos(K(\theta-\theta_0)^2 - K\theta_0^2 + \varphi), & \frac{\theta_0}{2} < \theta < \frac{3\theta_0}{2} \end{cases} \tag{10}$$

The synthetic antenna pattern can now be expressed in the following form

$$P(\theta_1) \sim \left| \int_{-\frac{3\theta_0}{2}}^{-\frac{\theta_0}{2}} G(\theta)W(\theta-\theta_1)\cos(K(\theta+\theta_0)^2 - K\theta_0^2+\varphi)\, e^{iK(\theta-\theta_1)^2} d\theta \right.$$
$$+ \int_{-\frac{\theta_0}{2}}^{\frac{\theta_0}{2}} G(\theta)W(\theta-\theta_1)\cos(K\theta^2+\varphi)\, e^{iK(\theta-\theta_1)^2} d\theta \tag{11}$$
$$\left. + \int_{\frac{\theta_0}{2}}^{\frac{3\theta_0}{2}} G(\theta)W(\theta-\theta_1)\cos(K(\theta-\theta_1)^2 - K\theta_0^2+\varphi)\, e^{iK(\theta-\theta_1)^2} d\theta \right|^2$$

Preliminary Evaluation

Taking the middle integral in equation (11) as an example, the product of the trigonometric and exponential factors may be expanded as follows:

$$\cos(K\theta^2+\varphi)\, e^{iK(\theta-\theta_1)^2} = \frac{1}{2} e^{iK\theta^2 + iK(\theta-\theta_1)^2 + i\varphi} + \frac{1}{2} e^{-iK\theta^2 + iK(\theta-\theta_1)^2 - i\varphi}$$

$$= \frac{1}{2} e^{i2K\theta^2 - i2K\theta_1\theta + iK\theta_1^2 + i\varphi} + \frac{1}{2} e^{-i2\theta_1\theta + iK\theta_1^2 - i\varphi} \tag{12}$$

Because the argument of the first term contains $i2K\theta^2$, it will oscillate rapidly with $\theta$ and will contribute little to the integral. On the other hand, $i2K\theta_1\theta$ in the argument of the second term will be very small for small $\theta_1$, and the term itself will be approximately a constant. The same observation can be made about the integrands of the other two integrals. On this basis, the integrals will be simplified by dropping from consideration all exponential factors with arguments containing terms of the form $i2K\theta^2$.

$$P(\theta_1) \sim \left| e^{iK\theta_1^2 - i\varphi} \left[ \int_{-\frac{3\theta_0}{2}}^{-\frac{\theta_0}{2}} G(\theta) W(\theta-\theta_1) e^{-i2K(\theta_1+\theta_0)\theta} d\theta \right.\right.$$

$$+ \int_{-\frac{\theta_0}{2}}^{\frac{\theta_0}{2}} G(\theta) W(\theta-\theta_1) e^{-i2K\theta_1\theta} d\theta \qquad (13)$$

$$\left.\left. + \int_{\frac{\theta_0}{2}}^{\frac{3\theta_0}{2}} G(\theta) W(\theta-\theta_1) e^{-i2K(\theta_1-\theta_0)\theta} d\theta \right] \right|^2$$

In order to proceed further, specific functions must be assumed for the antenna pattern. This will be done in the next section.

## The Antenna Pattern

A variety of assumptions might be made for the antenna pattern. In general, it is desired to assume a form for which the integrals above may be evaluated and which also preserves the essential features of the real situation. To this end, the following antenna pattern is adopted:

(1) A main beam is assumed with a Gaussian shape. It will normally be supposed that the beamwidth is small compared to the angle .

(2) A constant side lobe level is assumed without any lobe structure.

This assumed antenna pattern may be expressed as

$$G(\theta) = (1-\alpha) e^{-\frac{\theta^2}{.36\beta^2}} + \alpha \qquad (14)$$

$\beta$ = antenna beamwidth

$\alpha$ = average side lobe level

The form of this antenna pattern is illustrated in figure 1 for

$$\alpha = .01 \sim -20\ db .$$

## Further Evaluation

The antenna pattern adopted allows a relatively simple evaluation of the integrals in equation (14). The weighting function, W( ), is made

identical to the main beam portion of the antenna pattern. Because $\Theta_o$ is appreciably larger than a beamwidth, the contribution of the main beam portion of the antenna pattern may be neglected in the first and third integrals. Similarly, because of the localized nature of the functions $G(\Theta)$ and $W(\Theta - \Theta_1)$, the integrals may be approximated by extending their limits to arbitrarily large values. With these substitutions and modifications, equation (13) may be expressed as follows:

$$P(\theta_1) \sim \left| e^{iK\theta_o^2 - i\varphi} \left[ (1-\alpha) \int_{-\infty}^{\infty} e^{-\frac{\theta^2 + (\theta-\theta_1)^2}{.36\beta^2} - i2K\theta_1\theta} d\theta + \alpha \int_{-\infty}^{\infty} e^{-\frac{(\theta-\theta_1)^2}{.36\beta^2} - i2K\theta_1\theta} d\theta + \alpha \int_{-\infty}^{\infty} e^{-\frac{(\theta-\theta_1)^2}{.36\beta^2} - i2K(\theta_1+\theta_o)\theta} d\theta + \alpha \int_{-\infty}^{\infty} e^{-\frac{(\theta-\theta_1)^2}{.36\beta^2} - i2K(\theta_1-\theta_o)\theta} d\theta \right] \right|^2 \quad (15)$$

Carrying out the indicated operations.

$$P(\theta_1) \sim \left| e^{-i\varphi} \left[ \frac{1}{\sqrt{2}}(1-\alpha) e^{-\frac{\theta^2}{.12\beta^2} - (.045)(2K\beta\theta_1)^2} + \alpha e^{-iK\theta_1^2 - (.09)(2K\beta\theta_1)^2} + \alpha e^{-iK\theta_1^2 - i2K\theta_o\theta_1 - (.09)(2K\beta(\theta_1+\theta_o))^2} + \alpha e^{-iK\theta_1^2 + i2K\theta_o\theta_1 - (.09)(2K\beta(\theta_1-\theta_o))^2} \right] \right|^2 \quad (16)$$

The first two terms peak at $\Theta_1 = 0$ while the last two terms peak at $\Theta_1 = -\Theta_o$ and $\Theta_1 = \Theta_o$, respectively. Because these terms are disjoint or non-overlapping, their absolute values may be computed separately. It may also be noted that $\theta_1^2/.12\beta^2 << (.045)(2K\beta\theta_1)^2$ so that the first of these terms may be neglected. Performing these simplifying operations yields

$$P(\theta_1) \sim \begin{cases} \alpha^2 e^{-(.18)(2K\beta(\theta_1+\theta_o))^2}, & \theta_1 \approx -\theta_o \\ e^{-(.09)(2K\beta\theta_1)^2} \left[ \frac{1}{\sqrt{2}}(1-\alpha) + \alpha e^{-(.045)(2K\beta\theta_1)^2} \right], & \theta_1 \approx 0 \\ \alpha^2 e^{-(.18)(2K\beta(\theta_1-\theta_o))^2}, & \theta_1 \approx \theta_o \end{cases} \quad (17)$$

For computational purposes, these results are most conveniently expressed in terms of the synthetic beamwidth, $B$ .

$$B = \frac{1}{.36K\beta} \tag{18}$$

$$P(\theta_1) \sim \begin{cases} \alpha^2\left(e^{-\frac{(\theta_1+\theta_0)^2}{.36B^2}}\right)^2, & \theta_1 \approx -\theta_0 \\ e^{-\frac{\theta_1^2}{.36B^2}}\left[\frac{1}{\sqrt{2}}(1-\alpha)+\alpha\left(e^{-\frac{\theta_1^2}{.36B^2}}\right)^{1/2}\right], & \theta_1 \approx 0 \\ \alpha^2\left(e^{-\frac{(\theta_1-\theta_0)^2}{.36B^2}}\right)^2, & \theta_1 \approx \theta_0 \end{cases} \tag{19}$$

The synthetic beam pattern defined by this expression has been computed and plotted in figures 2 and 3 for the two cases $\alpha = .1$ and $.01$ corresponding to -10db and -20db side lobe skirts. In figure 2, the pattern without side lobe skirts is indicated by a dashed curve. In figure 3, the difference between the main lobe pattern with and without side lobe skirts is not detectable.

Discussion

An analysis has been performed to determine the relation between side lobe energy in the physical antenna beam and the structure of the synthetic beam pattern in a side-looking doppler radar. A number of assumptions were made in order to simplify the analysis as much as possible while still retaining the essential features of the problem. The major assumptions adopted were:

(1) An antenna pattern is assumed to consist of a Gaussian main lobe plus a constant side lobe skirt. This differs from reality to some extent in that the side lobe power is not localized in lobes but is spread out uniformly. As long as the magnitude of the skirt is equal to the magnitude of the primary side lobes of an actual antenna, this deficiency should not be significant. In fact, the case analyzed should provide pessimistic estimates.

(2) It is assumed that the processor employs a variable density weighting mask matched to the main beam pattern of the antenna. This weighting function materially aids in reducing the side lobe power in the synthetic beam pattern. Such a mask is an essential feature of an optimum system, although not all actual processors employ them.

(3) In an optical processor, there will be two secondary foci in image space besides the primary focus. It was assumed that all power associated with these secondary foci could be neglected. This was essentially what was being done in the discussion relating to equation (12). In an actual processor, special provisions are made to block out this power.

The final result in the form of a mathematical expression describing the synthetic beam pattern is given in equation (19). Numerical results are plotted in figures 2 and 3 for antenna side lobe skirts of -10db and -20db. In both cases, the synthetic main beam pattern with and without antenna side lobe skirts is practically undisturbed. The synthetic pattern side lobes at angular equivalents of the prf have magnitudes which are close to the square of the antenna skirt power. That is, these synthetic pattern side lobes are close to -20db and -40db, respectively.

The following conclusions were drawn from these results:

(1) The effects of antenna side lobes appear to be much less important than previously thought. In particular, antenna side lobes as large as -10db seem to have a negligible effect on the synthetic main beam.

(2) More important than the primary antenna side lobes is the antenna side lobe power in the neighborhood of the angular equivalents of prf harmonics. This power produces definite side lobes in the synthetic pattern. These synthetic pattern side lobes are quite small, however. If the antenna pattern skirt power is -10db, then the synthetic pattern side lobes will be close to -20db. Synthetic pattern side lobes of -20db are close to the limit which can be achieved in suppressing synthetic pattern side lobes due to vehicle motion disturbances.

One question not considered in this analysis which might be of significance in specifying antenna side-lobe requirements is the effect of non-linearities in the signal processor. It was essentially assumed that the recording and processing operations were linear. The dynamic range of the medium upon which the raw data is recorded is normally rather marginal. The dynamic range required is directly proportional to the antenna side lobe power. Thus, with large side lobes there may be substantial intermodulation on the raw data record. It is quite possible that this phenomenon is dominant in determining side lobe specifications. Thus, for a more complete story, the analysis in this memorandum should be supplemented by a further study of the effects of processor non-linearities.

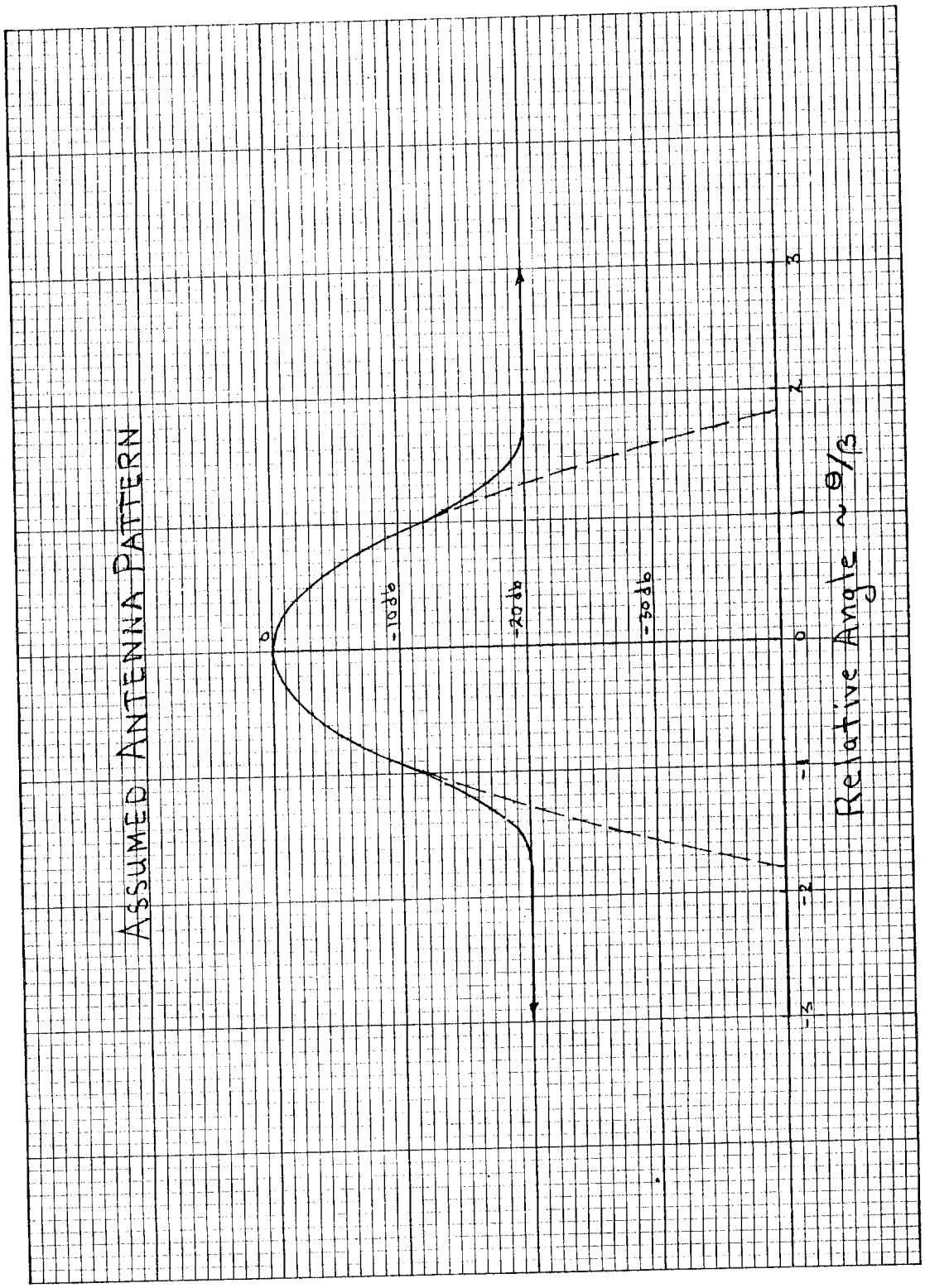


Figure 1

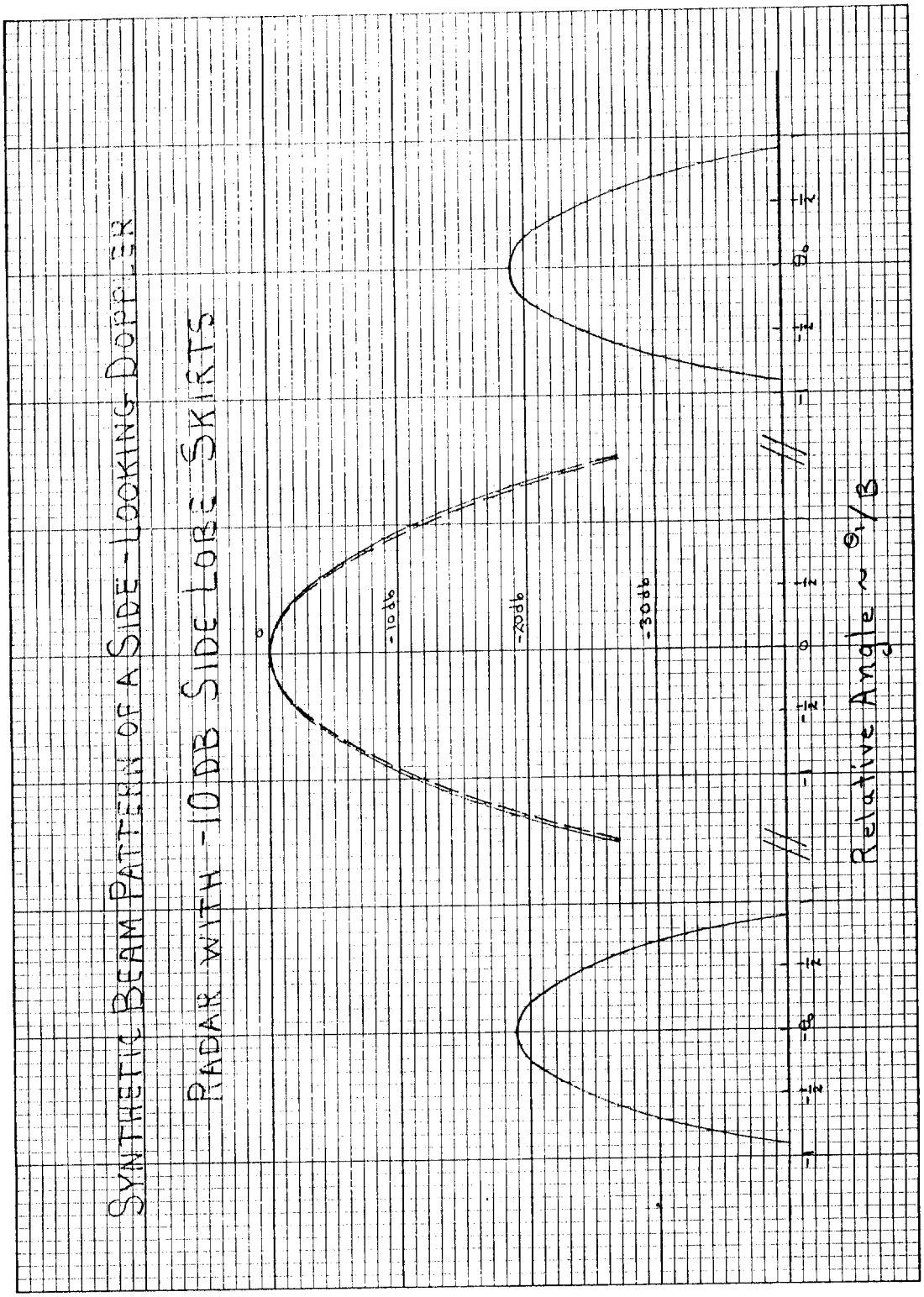


Figure 2

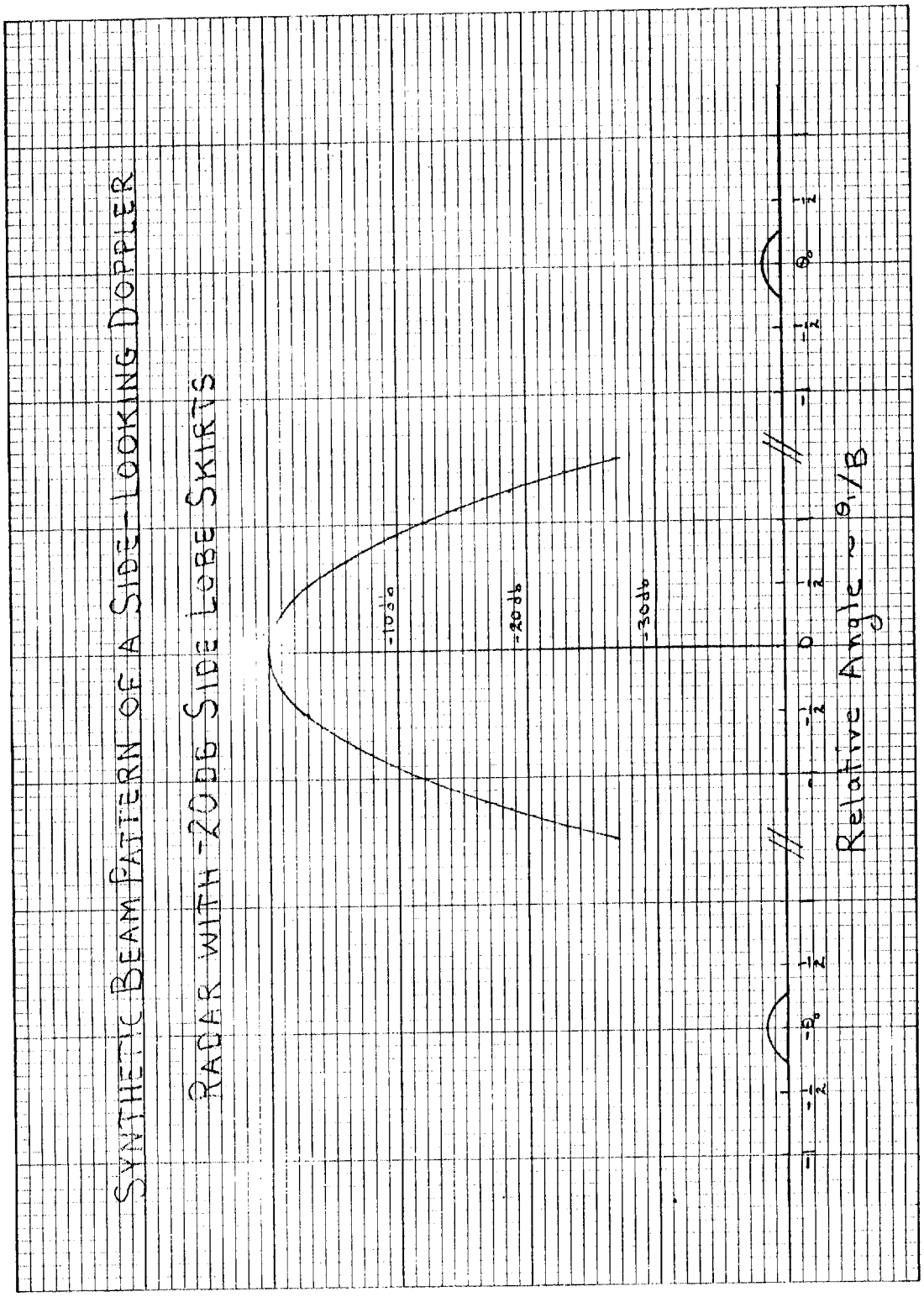


Figure 3